Aeolian Research 24 (2017) 81–91

Contents lists available at ScienceDirect

Aeolian Research

journal homepage: www.elsevier.com/locate/aeolia

The characterization of haboobs and the deposition of dust in Tempe, AZ from 2005 to 2014

Jershon Dale Eagar [a], Pierre Herckes [a], Hilairy Ellen Hartnett [a,b,*]

[a] School of Molecular Sciences, Arizona State University, PO Box 871604, Tempe, AZ 85287-1604, United States
[b] School of Earth and Space Exploration, Arizona State University, PO Box 876004, Tempe, AZ 85287-6004, United States

ARTICLE INFO

Article history:
Received 16 June 2016
Revised 21 November 2016
Accepted 21 November 2016
Available online 23 December 2016

Keywords:
Haboob
Dust storm
Dry deposition
Particulate matter
PM_{10}
TSP

ABSTRACT

Dust storms known as 'haboobs' occur in Tempe, AZ during the North American monsoon season. This work presents a catalog of haboob occurrence over the time period 2005–2014. A classification method based on meteorological and air quality measurements is described. The major factors that distinguish haboobs events from other dust events and from background conditions are event minimum visibility, maximum wind or gust speed, and maximum PM_{10} (particulate matter with aerodynamic diameters of 10 μm or less) concentration. We identified from 3 to 20 haboob events per year over the period from 2005 to 2014. The calculated annual TSP (total suspended particulate) dry deposition ranged from a low of 259 kg ha^{-1} in 2010 to a high of 2950 kg ha^{-1} in 2011 with a mean of 950 kg ha^{-1} yr^{-1}. The deposition of large particles ($PM_{>10}$) is greater than the deposition of PM_{10}. The TSP dry deposition during haboobs is estimated to contribute 74% of the total particulate mass deposited in Tempe.

1. Introduction

During the North American monsoon season Phoenix, Arizona is reported to experience 2–7 dust storms per year (Raman et al., 2014). Metropolitan Phoenix is a semiarid urban area with a population of 4.2 million (U.S. Census Bureau, 2013); the region has low annual precipitation ranging from 83 to 240 mm yr^{-1}, and high temperatures with an average of 61 days per year exceeding 40 °C (U.S. NOAA, 2015). The monsoon season is now defined by the National Weather Service (NWS) as June 15 to September 30 (similar to the 'hurricane season'; U.S. NWS, 2016); it is characterized by a change in the general upper atmosphere circulation and an average dew point >12.7 °C. The most intense kind of dust storms Phoenix experiences are fostered by monsoon weather through the interaction of atmospheric water and sunlight. In the vicinity of Phoenix, thunderstorm clouds build during the day as moisture-laden air aloft from the Gulf of Mexico and the Pacific Ocean (Sorooshian et al., 2011) is energized by sunlight and rises within the clouds. In the evening, the supply of heated, moist air decreases and there is a net downward movement of moisture as precipitation. Over the semiarid desert, the falling hydrometeors evaporate significantly before reaching the surface; this process cools the surrounding air, causing it to become denser and to displace the dry air below. These powerful downdrafts can produce high winds and turbulent convection over the landscape. These thunderstorm outflows can result in a particular kind of dust storm: an advancing wall of dust hundreds of meters high and tens of kilometers long known as a haboob, from the Arabic *habūb* 'blowing furiously/strong wind' (see Fig. 1 and Fig. 2; Idso, 1976; Idso et al., 1972; Sutton, 1925).

Haboobs occur in only a few parts of the world, including northern Africa (Roberts and Knippertz, 2012; Sutton, 1925), the Arabian Peninsula (Membery, 1985; Miller et al., 2008), and northwest India (there known as *kālī andhī* or *andhī* 'darkening, blinding storm'; Goudie and Middleton, 2000; Joseph, 1982; Joseph et al.,

Abbreviations: AQS, United States Environmental Protection Agency's Air Quality System; ADEQ, Arizona Department of Environmental Quality; BLDU, blowing dust; $c(PM_{10})$, mass concentration of PM_{10}; $c(PM_{2.5})$, mass concentration of $PM_{2.5}$; c(TSP), mass concentration of TSP; DS, dust storm; DU, widespread dust; EPA, United States Environmental Protection Agency; HZ, haze; $J_d(PM_{10})$, PM_{10} dry deposition flux; J_d(TSP), TSP dry deposition flux; KPHX, weather station at Phoenix Sky-Harbor International Airport; MADIS, Meteorological Assimilation Data Ingest System; MCAQ, Maricopa County Air Quality; METAR, Meteorological Terminal Air Report; MFCD, Maricopa County Flood Control District; NAAQS, United States National Ambient Air Quality Standards; NOAA, United States National Oceanic and Atmospheric Administration; NWS, United States National Weather Service; QCLC, Quality Controlled Local Climatological Data; SQ, squall; TS, thunderstorm; *VIS*, visibility; v_{WG}, wind and/or gust speed; WBAN, United States Weather-Bureau-Army-Nav.

* Corresponding author at: School of Earth and Space Exploration, Arizona State University, PO Box 876004, Tempe, AZ 85287-6004, United States.
E-mail address: h.hartnett@asu.edu (H.E. Hartnett).

http://dx.doi.org/10.1016/j.aeolia.2016.11.004
1875-9637/

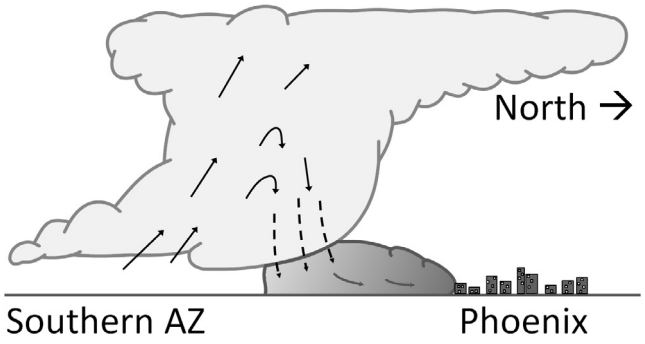

Fig. 1. Conceptual diagram of haboob initiation in Arizona, including a convective thunder storm (anvil cloud) and down drafts (dashed arrows) that push a wall of dust ahead of the storm. Gray shading of the haboob is meant to emphasize the dust font. Note: Not all haboobs originate south of Phoenix and the diagram is not to scale.

1980). In the US, haboobs have been reported in Arizona and Texas (Brazel and Nickling, 1986; Chen and Fryrear, 2002; Idso et al., 1972; Warn and Cox, 1951). In Arizona, haboobs can substantially decrease visibility to less than 1 km (Nickling and Brazel, 1984). Wherever haboobs occur, they are quite intense relative to other types of dust events (Roberts and Knippertz, 2012) and have comparatively short lifetimes of 1–4 h in any single location (Brazel and Nickling, 1986; Sutton, 1925).

1.1. Impact on air quality

Haboobs can have a significant impact on the amount of atmospheric particulate matter (PM) in the metropolitan Phoenix area (Clements et al., 2014, 2016; Lei and Wang, 2014). Particulate matter is classified by size fractions; PM_{10} and $PM_{2.5}$ are particulate matter with aerodynamic diameters of $\leqslant 10\,\mu m$ and $\leqslant 2.5\,\mu m$, respectively. The size of PM determines the extent of penetration into the respiratory tract and therefore the adverse health risk: PM_{10} can penetrate to the bronchi passages while the finer and more hazardous fraction, $PM_{2.5}$, is able to penetrate fully into the alveolar recesses of the lungs (WHO, 2006). Their mass concentrations, $c(PM_{10})$ and $c(PM_{2.5})$ respectively, both increase during haboobs; peak $c(PM_{10})$ can be in the thousands of $\mu g\,m^{-3}$ for several hours and $c(PM_{2.5})$ increases although to a somewhat lesser extent (*e.g.*, tens to hundreds of $\mu g\,m^{-3}$; Clements et al., 2013; Lei and Wang, 2014). The U.S. National Ambient Air Quality Standards (NAAQS) are 12 $\mu g\,m^{-3}$ for $c(PM_{2.5})$ and 150 $\mu g\,m^{-3}$ for $c(PM_{10})$ over a 24-h period (U.S. Environmental Protection Agency (EPA), 2013). High haboob-derived PM concentrations which exceed the EPA standards are typically excluded from regulatory decisions regarding NAAQS compliance since they are high-wind, natural-events that are "not reasonably controllable or preventable" and which overwhelm even stringent dust control measures (ADEQ, 2015; U.S. EPA, 2006, 2007).

Besides the impact on air quality, another impact of haboobs is particle deposition. In the early 1970s, rooftop dust deposition in Tempe was reported to be 540 $kg\,ha^{-1}\,yr^{-1}$, 12% of which was attributed to two haboobs (Péwé et al., 1981). Particle deposition in semiarid regions of southern California and Nevada (which do not experience haboobs) has been reported to be substantially lower, 20–200 $kg\,ha^{-1}\,yr^{-1}$, over the period 1983–2000 (Reheis, 2006).

Identification of haboobs in metropolitan Phoenix from historical data can be challenging since meteorological and radar records often are inadequate in temporal and spatial resolution to capture these short-lived phenomena (Raman et al., 2014). Reliance upon visibility and wind speed data alone can lead to false-positive haboob identifications since these events can occur with several meteorological phenomena. Recent high-resolution modelling efforts have also shown that it is possible to predict the timing and location of haboob events and have presented results simulating a particularly large haboob that occurred in July of 2011 (Vukovic et al., 2014). The METAR (Meteorological Terminal Air Report) weather condition codes provide dust information (*e.g.*, BLDU, blowing dust) but do not distinguish between general dust events and the more intense haboobs. Given the sparse data on dust deposition in the southwestern US, and the difficulty of identifying past haboob events, the magnitude of annual haboob deposition and the impact of that dust on urban ecosystems

Fig. 2. Photograph from an airplane of a haboob advancing northward in Tempe, AZ on August 25, 2015; photo credit: A. Anbar.

is not well known. However, it is likely that as the Phoenix population continues to grow, changes in land use will affect the potential for monsoon events to resuspend and transport dust in and around metropolitan Phoenix.

This work identified and characterized haboobs in Tempe, AZ over the period 2005–2014. Air quality impacts were documented and temporal changes in haboob frequency and intensity were investigated. A computational model was used to estimate particle deposition in Tempe. This work is of limited spatial scope since it reports the development of a systematic classification of haboobs. This work exceeds prior location-specific libraries of haboob events in that it employs air quality and meteorological data in haboob classification.

2. Material and methods

2.1. Retrieval of meteorological and air quality records

Metropolitan Phoenix covers a large area (37,700 km^2) and as such, there is heterogeneity in dust deposition throughout the area (Péwé et al., 1981). To maintain consistency with older studies, the weather station at the Phoenix Sky Harbor International Airport (KPHX; see Fig. 3) was selected for dust event identification. The KPHX station has weather records back to 1930 and was also the location used in the older published dust storm studies (*e.g.*, Brazel and Nickling, 1986). KPHX is also proximal to ASU's Tempe campus as well as to a variety of long-term ecological study sites (*e.g.*, Ball and Guevara, 2015; Bateman et al., 2015; Davis et al., 2015; Giraudeau et al., 2015) for which the deposition predictions of this work could augment the existing research. We retrieved KPHX hourly, quality-controlled local climatological data from 2005 to 2014 (U.S. NOAA, 2015). Haboob classifications were applied using $c(PM_{10})$ data from two air quality stations that were selected in proximity to KPHX, namely, Central Phoenix (CP) and Tempe (TE); see Table 1 and Fig. 3 (U.S. EPA, 2015).

Four additional weather stations in Tempe were used to confirm the presence of haboob dust, namely AN014, MAGC, SA31, and SRP01 (MesoWest, 2015). Two additional air quality sites were chosen to better distinguish high smog events from dust events, namely DI and VEL (see Table 1 and Fig. 3; U.S. EPA, 2015).

2.2. Historical haboob identification and categorization

Hourly weather and air quality data from KPHX for the years 2005–2014 were searched for dust event signatures (see flowchart in Fig. S1). A dust event was considered a meteorological condition of reduced visibility (*VIS*), elevated wind and/or gust speed (v_{WG}), and elevated $c(PM_{10})$. To begin, a preliminary list was generated for hours in which any of the following occurred: minimum $VIS < 16$ km (<10 mi), maximum $v_{WG} > 17$ m s^{-1} (>40 mi h^{-1}), a 1 h average $c(PM_{10}) \geqslant 200$ μg m^{-3}, or the occurrence of dust-related METAR weather condition codes (*e.g.*, BLDU, blowing dust; DS, dust storm; DU, widespread dust; HZ, haze; TS, thunderstorm; SQ, squall). The hours identified were then grouped into events. Events were assumed to be separate when the weather and air quality signatures returned or were 'reset to fair weather conditions' for at least 6 h. There were 422 events which met the preliminary criteria. Some confounding factors which can cause low air visibly were heavy rain, fog, and smog. To avoid false-positives, each event was assessed individually for coincident *VIS* drops, v_{WG} spikes, $c(PM_{10})$ spikes, and appropriate METAR weather condition codes. After removing high smog episodes, fog, heavy rain, and thunderstorms without dust, there were 266 candidate dust events that remained.

There is a characteristic meteorological signature that accompanies thunderstorm outflows and, therefore, haboobs (Idso et al., 1972). This signature includes a rapid increase in humidity and air pressure, a rapid decrease in air temperature, and a spike in $c(PM_{10})$, generally $\geqslant 200$ μg m^{-3} for 1–3 h (see Fig. S2). The individual dust events were inspected for this signature and were categorized as either haboobs or 'other dust'. Non-haboob dust events had longer durations (*i.e.*, 3–12 h) of elevated $c(PM_{10})$ without abrupt changes in temperature, humidity, and pressure. Mild haboobs with visibility $VIS > 11.3$ km (>7 mi) were grouped with the 'other dust' since they were more difficult to positively identify. Following data review, 96 haboob events with $VIS \leqslant 11.3$ km ($\leqslant$7 mi) were identified for the years 2005–2014 (see Table S1 for list). Photographic evidence for haboob events early in this period was often not available. In the latter portion of the 2005–2014 period, social media reports of these events were more common and of the 96 haboob events, 43 were confirmed by photographs of advancing 'walls' of dust obtained from the local press, social media, or web camera records.

2.3. Dry deposition model

Dry deposition in Tempe was estimated using a model similar to that of Sauret et al. (2009). The sedimentation velocities (v_s) for 36 particles sizes (aerodynamic diameters from 0.1 to 320 μm) were calculated with Eq. (1), where ρ_p is the particle density (1.7×10^6 g m^{-3}), $d_{p,j}$ is the jth aerodynamic particle diameter, g is the gravitational constant, $C_{f,j}$ is the diameter-specific particle Cunningham factor (*i.e.*, a sliding factor), and η_{air} is the dynamic viscosity of air:

$$v_{s,j} = d_{p,j}^2 \rho_p g C_{f,j} / (18 \eta_{air}) \quad (1)$$

$C_{f,j}$ was calculated as a function of $d_{p,j}$ where λ_p is the particulate mean free path in air (an estimated constant value of 0.066 μm). Calculated $C_{f,j}$ agreed with values given in Sauret et al. (2009) and Seinfeld and Pandis (2006):

$$C_{f,j} = 1 + \frac{\lambda_p}{d_{p,j}} (2.514 + 0.8 e^{-0.55 d_{p,j}/\lambda_p}) \quad (2)$$

Diameter specific Reynolds numbers (Re_j) were calculated as a function of $d_{p,j}$ where ρ_{air} is the density of air:

$$Re_j = \rho_{air} v_{s,j} d_{p,j} / \eta_{air} \quad (3)$$

For particle sizes where the Re_j was >1, drag was included in the sedimentation velocity calculation and $v_{s,j}$ from Eq. (4) was used in deposition calculations (Seinfeld and Pandis, 2006):

$$v_{s,j} = d_{p,j}^{8/7} \left(\frac{4}{55.5} g \rho_p C_{f,j} \right)^{5/7} \Big/ \left(\rho_{air}^{2/7} \eta_{air}^{3/7} \right) \quad (4)$$

A static value of η_{air} is not adequate for metropolitan Phoenix where diurnal temperatures differ by an average of 12 °C (22 °F) with a range of 2–22 °C (4–39 °F; U.S. NOAA, 2015). During thunderstorm outflows, the temperature and pressure both change, causing η_{air} to decrease and therefore v_s to increase by as much as 5% in 1–2 h (*e.g.*, 2 August 2005 in Fig. S3). Hourly η_{air} and ρ_{air} were calculated using Mathematica 10 (Mathematica, 2015a, 2015b) as a function of KPHX dry bulb air temperature and air pressure. Values for η_{air} and ρ_{air} varied by time of day and by season, with η_{air} ranging from 0.0171 to 0.0195 g m^{-1} s^{-1} and ρ_{air} ranging from 1.05 to 1.27 kg m^{-3} (see Figs. S3 and S4).

The dry deposition flux (J_d) was calculated using Eq. (5), where $v_{s,i,j}$ is the sedimentation velocity of PM with diameter j during a time interval i, x_j is the diameter-specific mass fraction, t_j is the length of a measurement interval (*i.e.*, 1 h), and $c(PM_{10})_i$ is the PM_{10} mass concentration during the interval:

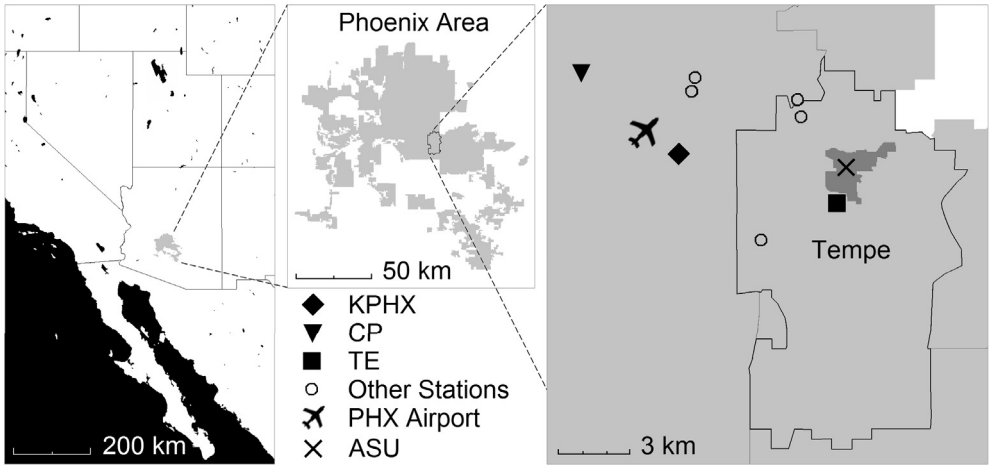

Fig. 3. Map of the southwest U.S. (left) with gray shading indicating metropolitan Phoenix, an enlargement of metropolitan Phoenix (middle) with the City of Tempe's boundaries as a black line, and a detail map of the City of Tempe (right) with the ASU campus indicated by an '×' and dark gray shading. The local meteorological stations and air quality system monitoring sites are indicated by symbols. The filled diamond, triangle, and square indicate locations of the KPHX, CP, and TE sites, respectively; open circles indicate the locations of other meteorological stations and air quality sites, including: MAGC, SA31, SRP01, DI, and VEL. The Phoenix Sky Harbor International Airport is indicated by a small plane. (See Table 1 for full station names and station abbreviations in the legend.)

Table 1
Summary of public data and sources used to categorize haboob events.

Abbreviation	Date range	Data type	Station name	Station ID	Provider
KPHX	2005-Present	QCLCD†	Phoenix Sky Harbor International Airport	WBAN 23,183‡	U.S. Weather Bureau¤
	1930-Present	Meteorological	Phoenix Sky Harbor International Airport		
CP	1985-Present	$c(PM_{10})$^	Central Phoenix	AQS* 04-013-3002	MCAQ#,@
	1965-Present	Gases	Central Phoenix		
TE″	2012-Present	$c(PM_{10})$, $c(PM_{2.5})$¢	Tempe	AQS 04-013-4005	MCAQ
	2000-Present	Gases	Tempe		
DI	2014-Present	$c(PM_{2.5})$, Gases	Diablo	AQS 04-013-4019	MCAQ
VEL	1989-Present	Gases	Vehicle Emissions Lab	AQS 04-013-9998	ADEQ£,@
	2003-Present	Nephelometry	Vehicle Emissions Lab		
AN014″	2010–2014	Meteorological	Tempe	AN014	MCAQ
SA31	2014–2015	Meteorological	Tempe SA31	SA31	MADIS¶,§
SRP01	2013-Present	Meteorological	SRP	SRP01	Salt River Project§
MAGC	2005-Present	Meteorological	GateWay Community College	MAGC	MFCD¥,§

Notes: †, QCLCD: hourly quality controlled local climatological data; ‡, WBAN: Weather-Bureau-Army-Navy; ¤, http://www.ncdc.noaa.gov/qclcd; ^, $c(PM_{10})$: PM_{10} mass concentration; *, AQS: U.S. Environmental Protection Agency Air Quality System; #, MCAQ: Maricopa County Air Quality; @, http://aqs.epa.gov/api; ″, Stations TE and AN014 are co-located; ¢, $c(PM_{2.5})$: $PM_{2.5}$ mass concentration; £, ADEQ: Arizona Department of Environmental Quality; ¶, MADIS: Meteorological Assimilation Data Ingest System; §, http://mesowest.utah.edu; ¥, MFCD: Maricopa County Flood Control District.

$$J_{\text{dry}} = \sum_{i=1}^{n}\left[t_i c(\text{PM}_{10})_i \cdot \sum_{j=0.1\mu\text{m}}^{320\mu\text{m}}[v_{s,ij}x_j]\right] \quad (5)$$

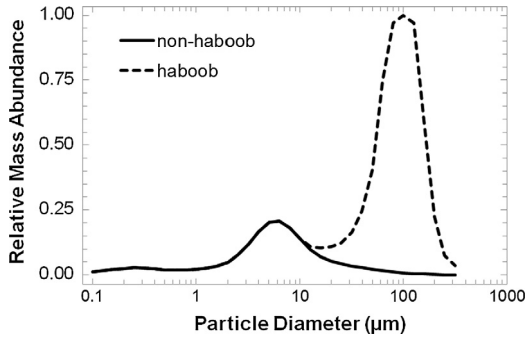

Fig. 4. Composite PM mass distributions for haboob and non-haboob periods. The haboob distribution had a $\frac{PM_{10}}{TSP}$ mass ratio of 0.20. The non-haboob distribution was the average of literature mass distributions (Sauret et al., 2009; Seinfeld and Pandis, 2006). The haboob and the non-haboob distributions differed only for particle aerodynamic diameters >10 μm. Much of the mass in the haboob distribution was comprised of large particles. See Figs. S5 and S6 for a more detailed explanation.

The PM mass distributions were calculated from distributions reported in the literature (see Fig. 4). During non-haboob time periods, x_j was the average of two distributions (Sauret et al., 2009; Seinfeld and Pandis, 2006). Values of x_j were scaled so that the entire PM_{10} mass fraction was unity:

$$\sum_{j=0.1\mu\text{m}}^{10\mu\text{m}} x_j = 1 \quad (6)$$

During haboob time periods, we employed a distinct mass distribution based on dust storm distributions from the literature (Box et al., 2010; Chen and Fryrear, 2002; Gillette et al., 1978; O'Hara et al., 2006). During dust events such as haboobs, much of the particulate mass is comprised of $PM_{>10}$ (PM with $d_p > 10$ μm). The mass ratio of PM_{10} to the total suspended particulates (TSP), or $\frac{PM_{10}}{TSP}$, has often been reported to be <0.3 during large dust storms (see Table 2) meaning that there was more mass of particles with $d_p > 10$ μm than the mass with $d_p \leqslant 10$ μm. Due to differences in sampling methodologies as well as to the quite variable intensity of dust storms, literature particle mass distribution ratios vary somewhat widely (Table 2). Some $\frac{PM_{10}}{TSP}$ ratios are listed as upper bounds in Table 2 as a consequence: $PM_{>18}$ was not reported

Table 2
Dust storm mass distribution ratios and deposition.

Location	$\frac{PM_{10}}{TSP}$¥	J_d(TSP)¢, kg ha^{-1}	Sample duration	Reference
USA				
Phoenix	n/a	540 yr^{-1}	Annual	Péwé et al. (1981)
Western Texas	0.06*,¤	850 h^{-1}	1 haboob	Chen and Fryrear (2002)
Colorado and Kansas	0.28; 0.30¤	n/a	2 dust storms	Chepil (1957)
Northwest Texas	0.18–0.27*	210–790 h^{-1}	3 dust storms	Gillette et al. (1978)
Pennsylvania	n/a	15.3, storm total	1 dust storm†	Miller (1934)
Southern California & Nevada	n/a	20–200 yr^{-1}	Annual	Reheis (2006)
Europe				
Ukraine	n/a	20–6940 mo^{-1}	4 weeks§	Shikula (1981)
Middle East				
Dead Sea, Israel	n/a	255–605 yr^{-1}	Annual	Singer et al. (2003)
Negev Desert, Israel	n/a	1100–2200 yr^{-1}	Annual	Goossens and Offer (1995)
Northern Africa				
Libya	<0.18 to <0.77‡	366–4210 yr^{-1}	Annual	O'Hara et al. (2006)
Western Chad	n/a	537 yr^{-1}@	Annual	Maley (1980)
Northern Nigeria	n/a	991 yr^{-1}	Annual	McTainsh (1980)
Northern Nigeria	<0.67‡	>850 yr^{-1}	1 dust season	Møberg et al. (1991)
Southwest Niger	n/a	1640–2120 yr^{-1}	Annual	Drees et al. (1993)
Australia and New Zealand				
Sydney, Australia	<0.85; <0.87*,^	n/a	2 dust storms	Box et al. (2010)
South Island, New Zealand	n/a	>710 to >6140 yr^{-1}	1 dust season	McGowan et al. (1996)

Notes: ¥, $\frac{PM_{10}}{TSP}$: mass ratio of PM_{10} to TSP; ¢, J_d(TSP): TSP dry deposition flux; *, ratio was estimated from histograms; ¤, average of 5–20 ft. sampler heights; †, originated in mid-west USA and traveled 2000 km; §, historically, the dust storms during the 4 weeks were unusually severe for the Ukraine; ‡, PM_{20} and $PM_{>20}$ were reported; @, calculated with dust density of 0.85 g cm^{-3}; ^, $PM_{>18}$ not reported.

(Box et al., 2010) or PM_{20} and $PM_{>20}$ were reported but not PM_{10} and $PM_{>10}$ (Møberg et al., 1991; O'Hara et al., 2006). The composite haboob mass distribution used in this study was identical to the non-haboob distribution for PM_{10}, but for $PM_{>10}$ the haboob x_j values were scaled with the mass ratio $\frac{PM_{10}}{TSP}$ such that Eq. (7) obtained:

$$\sum_{j>10\mu m}^{320\mu m} x_j = 1 - \frac{PM_{10}}{TSP} \quad (7)$$

Thus, the model utilized a particle mass distribution where much of the haboob TSP was $PM_{>10}$ $\left(\frac{PM_{10}}{TSP} = 0.20\right)$ while the background (non-haboob) TSP mass was primarily PM_{10} $\left(\frac{PM_{10}}{TSP} = 0.78\right)$. A more detailed discussion of the literature and composite distributions is given in Figs. S5 and S6. To avoid overestimation of deposition, the non-haboob mass distribution was used for mild haboob events (*i.e.*, *VIS* > 11.3 km) and for dust events lacking a clear meteorological signature of a convective thunderstorm outflow.

3. Results and discussion

3.1. Haboob occurrence, characteristics, and frequency

Most haboobs with *VIS* ⩽ 11.3 km (⩽7 mi) in Tempe over the period 2005–2014 occurred in the months of July and August, which exhibited median event frequencies of 4 and 2.5, respectively (Fig. 5). This timeframe coincides with the North American monsoon season and is in agreement with Brazel and Nickling's (1986) data for haboobs near Tempe from 1965 to 1980.

In Fig. 5, zero median dust event occurrences are indicated as the absence of a bar. In June, the mean annual precipitation was 0.05 mm. The summertime precipitation pattern and haboob modes are consequences of thunderstorm evolution and convective outflows. Haboobs do not necessarily require precipitation to occur, yet are intrinsically linked to the summer precipitation near metropolitan Phoenix. Thus, the most intense type of dust storm that occurs in Tempe, the haboob, is not only dependent upon relatively hot and dry surface conditions, but also requires significant sources of moisture from outside the region, such as the Gulf of Mexico and Gulf of California (Sorooshian et al., 2011). Haboobs do not coincide with the winter rainy periods since winter storms do not have the characteristics necessary to trigger haboob events (*e.g.*, convective outflow, surface temperatures, etc.).

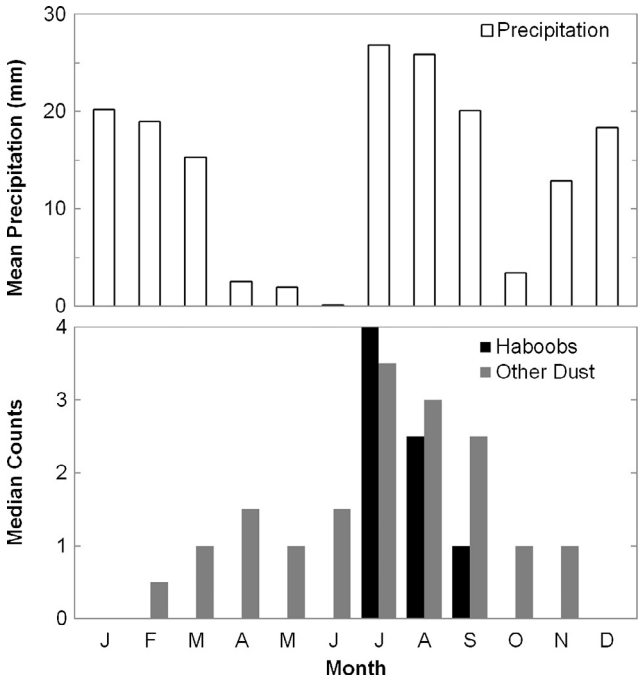

Fig. 5. Monthly mean precipitation (top) and median dust occurrence (bottom) in Tempe over the period 2005–2014. Haboobs were categorized as convective outflow events with minimum *VIS* > 11.3 km (7 mi). Other dust comprises events that failed to meet either the visibility or the meteorological criteria for haboobs. Precipitation was bimodal; rains during the North American monsoon season (July to September) coincided with haboobs while winter precipitation (November to March) coincided with few dust events.

The 'other dust' events category included unconfirmed haboobs, mild haboobs (*e.g.*, minimum *VIS* > 11.3 km), and dust caused by other meteorological phenomena such as cold fronts. 'Other dust' events occurred in most months of the year with a mode during the monsoon season due to the contribution of mild haboobs. The winter precipitation mode appeared to inhibit dust storms, as indicated by zero median dust event occurrences in December and January (see Fig. 5).

The number of haboobs and precipitation varied substantially from year to year over the period 2005–2014. Haboob occurrences ranged from 3 to 20 yr^{-1} with an annual average of 9.6 yr^{-1} (see Fig. 6). Cumulative annual precipitation (*i.e.*, total precipitation in a calendar year) ranged from 83 to 240 mm yr^{-1}, with an average of 166 mm yr^{-1}. Such year-to-year variation was also reported from 1965 to 1980 by Brazel and Nickling (1986) when the number of haboobs ranged from 1 to 19 yr^{-1}. In general, fewer haboobs occurred during 2005–2014 in years with greater annual precipitation, in agreement with Brazel (1989) and Holcombe et al. (1997). For example, in 2008 and 2010, Tempe received 240 and 230 mm yr^{-1} rain, respectively, and experienced 4 and 3 haboobs, respectively. In drier years, for example 2011 and 2012, Tempe received less rain, 118 and 109 mm yr^{-1}, respectively, and experienced 20 and 19 haboobs, respectively. However, the relationship between precipitation and haboobs in Tempe is complicated by the bimodality of annual precipitation and by many other factors unrelated to precipitation (*e.g.*, anthropogenic activity and land use changes; Macpherson et al., 2008). During the driest year of this study, 2009, Tempe received 83 mm of precipitation and experienced 7 haboobs, a below average number. The year 2009 was the only year investigated in this study when annual precipitation was below 100 mm. The simplest explanation of decreased haboob occurrence during 2009 is that it was a manifestation that summer precipitation and haboobs have a mutual source: thunderstorms. However, Goudie (1983) observed that global dust storm occurrence increased as precipitation decreased until reaching a 'hyperaridity' threshold, 100 mm yr^{-1}, below which dust storm occurrence decreased, which was speculated to be due to prior removal of wind-erodible soil, the formation of wind-stable desiccated surfaces, and/or a lack of moisture-associated, dust-storm-initiating weather patterns (*e.g.*, thunderstorms, frontal passage). Further investigation would be required to assess whether this hyperaridity threshold applies in central AZ. The bimodality of precipitation in Tempe as well as anthropogenic activity and land use change very likely also impact the specific relationship between haboob occurrence and precipitation.

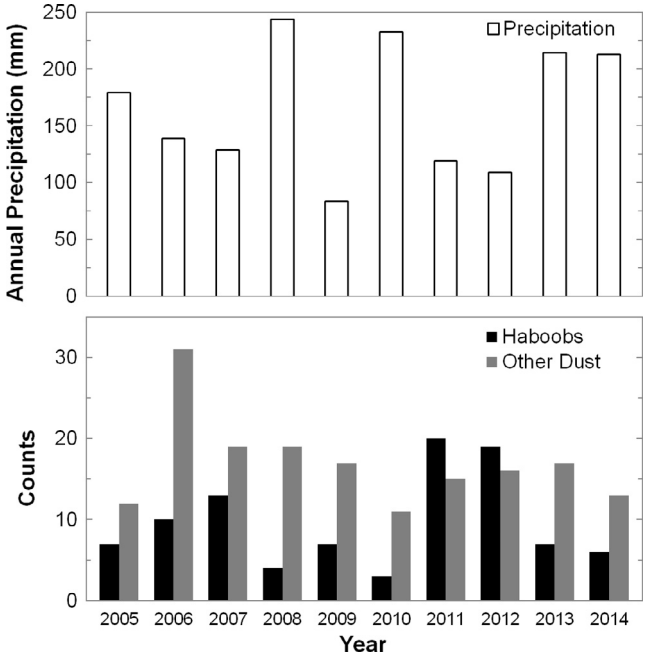

Fig. 6. The annual precipitation (by calendar year; top) and annual occurrence of dust events (bottom) in Tempe over the period 2005–2014. Haboobs were convective outflow events with minimum $VIS \leqslant 11.3$ km. 'Other dust' events failed to meet haboob visibility or meteorological criteria. There was significant year-to-year variation in precipitation and in haboob occurrence: 83–240 mm and 3–20 haboobs respectively.

The relationship between precipitation and haboobs in an urban environment is likely to be complex. Land use, land cover, and the disruption of stabilized soil surfaces are affected by a variety of human factors such as economic downturns (*i.e.*, decreased construction, agricultural, and recreational activities), dust mitigation efforts, and air quality regulations (Clements et al., 2014; Holcombe et al., 1997; Hyers and Marcus, 1981; Macpherson et al., 2008; Upadhyay et al., 2015). Precipitation from thunderstorms in this region is extremely heterogeneous and can also evaporate significantly before reaching the Earth's surface during the initiation of a haboob. The precipitation that reaches the ground may also occur far from Tempe and thus, would not be apparent in the Tempe precipitation records. Metropolitan Phoenix is a highly built–environment and the city has reservoirs that buffer against drought and canals that distribute water year-round. It is, as yet, unclear how much impact diminished precipitation really has on dust production in the area.

The systematic method used in this work provided robust classifications (see Fig. 7) with significant differences between the mean of haboobs and all other dust events for maximum v_{WG} ($p < 0.001$) as well as maximum $c(PM_{10})$ ($p < 0.001$). The mean v_{WG} of haboobs was >75% of other dust events (see Fig. 7) and the mean of haboob maximum $c(PM_{10})$, 884 μg m^{-3}, was larger than most (99th percentile) of the other dust events. All of the dust event peak $c(PM_{10})$ were larger than the background mean $c(PM_{10})$ of 33 μg m^{-3}. The differences in the mean minimum *VIS* of haboobs and other dust are a consequence, in part, of the visibility threshold employed in the classification method. Peak $c(PM_{10})$ in the hundreds or thousands of μg m^{-3} is relatively high yet it is sustained for only one or two hours, which may allow one to limit exposure to high PM by seeking shelter from the storm.

3.2. Comparison with literature classification methods

The classification method used in this work bears similarity to classifications previously applied in other U.S. locations. Hagen and Woodruff (1973) and Orgill and Sehmel (1976) identified dust storms from historical records based on 2 criteria: (1) when dust was reported and $VIS < 11.3$ km; or (2) when $11.3 \leqslant VIS \leqslant 14.5$ km and $v_{WG} > 5.4$ m s^{-1} (7 mi, 7–9 mi, and 12 mi h^{-1}, respectively). The present work did not employ a wind speed requirement to be considered a dust event. Nevertheless, nearly 97% of all dust events cataloged here had peak $v_{WG} > 5.4$ m s^{-1}. Notably, the past work of Hagen and Woodruff (1973) and Orgill and Sehmel (1976) did not distinguish between types of dust storms or report dust statistics specific to Phoenix.

Lei and Wang (2014) cataloged and characterized dust storms of many kinds (including haboobs) throughout the southwestern U.S. for 10 years. Their methodology did not specify a visibility threshold but was based on dust storms in the literature and in the media that had supporting evidence in meteorological and air quality records. Their method could not be used in Tempe to classify haboobs since there has been a dramatic increase in public awareness and social media attention in the last few years. Only classifying the publicized and media-reported events in Tempe

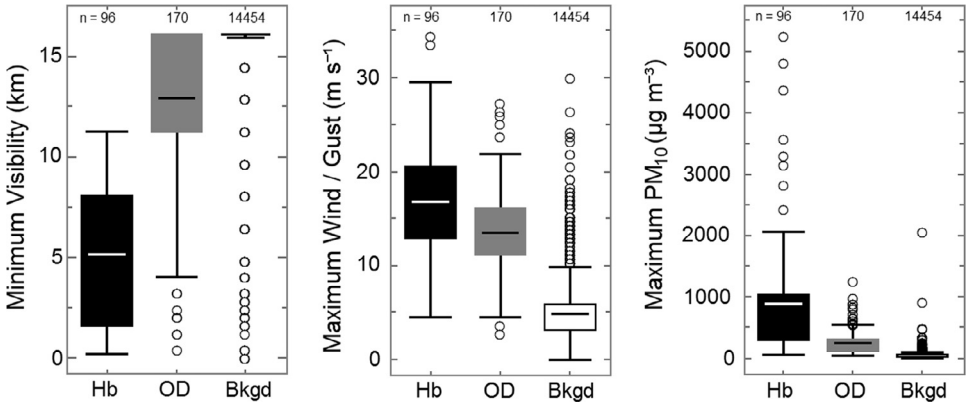

Fig. 7. Box plots summarizing basic characteristics of dust storms in Tempe for the period 2005–2014. Minimum visibility (left), maximum wind or gust speed (middle), and maximum PM_{10} concentration (right) are the major factors that distinguish haboobs events (Hb) from other dust events (OD) and background (Bkgd) conditions. The horizontal lines inside the boxes are mean values; the box boundaries are the 25th and 75th percentiles, respectively; the whiskers are the 10th and 90th percentiles, respectively; and the symbols are outliers. Haboobs with $VIS \leqslant 11.3$ km (7 mi) had much higher PM_{10} concentrations than 'other dust' events. Other dust includes those events that failed to meet the visibility and meteorological criteria for haboobs. The background data was divided into 6-h intervals and are the extrema for those time periods. Background data include periods of smog, fog, rain, and fair weather. The numbers above the box plots are the event counts.

would have introduced a significant bias toward very recent and/or large events.

It is possible to subdivide our haboob category based on intensity using the KPHX visibility data. Brazel and Nickling (1986) and Nickling and Brazel (1984) classified dust storms by storm type and by visibility in specific areas of Arizona, including Tempe. They employed visibility thresholds of $VIS \leqslant 1.6$ km (1 mi) as intense and $1.6 < VIS \leqslant 11.3$ km (1–7 mi) as moderate. Using their classification system, we identified 25 'intense' haboobs and 71 'moderate' haboobs during the time period 2005–2014. Another difference between the work of Brazel and Nickling and our current work was that they used four meteorological categories for dust while the current work used only two categories ('haboob' and 'other dust').

The Australian Meteorological Society visibility threshold for severe dust storms is $VIS \leqslant 0.2$ km and the threshold for moderate dust storms is <1 km (about 0.12 and 0.63 mi, respectively); higher visibility dust events are not considered storms but blowing dust episodes (O'Loingsigh et al., 2014). Using this classification system, we identified one 'severe' haboob and six 'moderate' haboobs in Tempe during the years 2005–2014. Indeed, the 'severe' haboob (5 July 2011) was quite exceptional in that it was larger than any haboob in the preceding 10 years (2001–2011) (Raman et al., 2014); this event caused power outages for ~10,000 customers, delayed airline flights, and received much attention even in the national press and social media (*e.g.*, Huffington Post, 2011). We included in our catalog haboobs of lesser intensity than a 'dust storm' by international standards because they are noteworthy and disruptive to the large population in metropolitan Phoenix, frequently exceeding the NAAQS 24-h $c(PM_{10})$ limit (150 µg m^{-3}; U.S. EPA, 2013). Moreover, these smaller haboob events also have high TSP deposition.

Land use in the area directly surrounding KPHX has changed substantially since the systematic categorization of haboobs in Tempe by Brazel and Nickling (1986). Areas that had extensive agricultural fields have been replaced with suburban and industrial development. An approximate boundary between urban and agricultural areas used to be 5–10 km south of KPHX but that has expanded to 15–20 km south of KPHX (Jenerette et al., 2001; Li et al., 2014; Maricopa County Assessor's Office, 2016). A direct comparison with the literature to determine whether the number and/or intensity of haboobs in metropolitan Phoenix has changed in since the mid-20th century will require additional locations beyond just the KPHX station and is thus beyond the scope of this paper. Additionally, the nearly one order of magnitude annual variation in haboob occurrences and the relatively short temporal coverage of the present work (10 years) further prevents a more robust temporal comparison.

3.3. Uncertainties in the deposition model and sensitivity analysis

The largest uncertainty in the deposition calculations is the mass distribution employed for haboob events since no measurements are available for the Phoenix area. It is known that uncertainty in particle mass distributions affects the accuracy of global and local deposition models (Lawrence and Neff, 2009). In the present work, the calculated deposition was found to increase by 700% between $\frac{PM_{10}}{TSP}$ ratios of 0.09 and 0.50 (data not shown). The ratio makes a significant difference since large particles deposit faster than small particles. There are some studies of dust storm particle mass distributions but diameter ranges are sometimes incomplete and the agreement between studies is somewhat limited (Box et al., 2010; Chen and Fryrear, 2002; Chepil, 1957; Gillette et al., 1978; Møberg et al., 1991; O'Hara et al., 2006; Singer et al., 2003). We anticipate that dust distributions will differ by location and dust source. Other differences are method related. Many different techniques for determining diameter specific PM mass distributions have been employed in the literature including: multi-stage impactor sampling (Box et al., 2010); sedimentation in air (Chen and Fryrear, 2002); sedimentation in aqueous solution (Møberg et al., 1991); sedimentation in chlorinated solvent (Chepil, 1957; Chepil and Woodruff, 1957); mechanical sieving (Chen and Fryrear, 2002); measurements with a phase-contrast light microscope (Gillette et al., 1978); and laser particle counters (O'Hara et al., 2006; Singer et al., 2003). Each method of particle size analysis differs in the range of particle sizes reliably quantified and the associated artifacts of analysis.

Our model employed $c(PM_{10})$ to estimate TSP deposition. $c(PM_{>10})$ is seldom reported due to the physical constraints of commercially available sampling equipment (*e.g.*, standard multistage high-volume samplers). This may be due to the fact that $PM_{>10}$ is not regulated as an air quality hazard. Since total suspended particle concentration, c(TSP) was not available in Tempe, a synthesized $\frac{PM_{10}}{TSP}$ mass ratio of 0.20 was used for haboobs; this value is within the range of values reported for other locations (see Table 2). A few studies in Northern Africa (Møberg et al., 1991; O'Hara et al., 2006) quantified PM_{20} and $PM_{>20}$ from which a $\frac{PM_{20}}{TSP}$ mass ratio

can be determined (Table 2). For these, the $\frac{PM_{10}}{TSP}$ mass ratios are estimated as upper bounds since $\frac{PM_{20}}{TSP} > \frac{PM_{10}}{TSP}$. Mass ratios derived from measurements in Australia are similarly given as upper bounds since $PM_{>18}$ was not measured (Box et al., 2010) and $\frac{PM_{10}}{PM_{>18}} > \frac{PM_{10}}{TSP}$.

It is likely that the $\frac{PM_{10}}{TSP}$ ratio would be lower for low visibility haboobs than for moderate visibility haboobs as the amount of large particles, $c(PM_{>10})$, would be higher. Since detailed and event-specific TSP mass distributions were not available, we employed 0.20 for all haboobs with *VIS* > 11.3 km (>7 mi). The calculated deposition of the 'other dust' events is likely an underestimate since the non-haboob PM mass spectrum was employed, which lacks a large particle ($PM_{>10}$) mode.

The measurement of $c(PM_{10})$ at the CP and TE air quality monitoring sites varied both in time and in magnitude. This was to be expected since thunderstorm outflows are directional and may not arrive at different locations throughout metropolitan Phoenix at the same time. In an attempt to minimize these differences, the meteorological and air quality sites used were chosen to be the closest to a reference point: the ASU Tempe campus (Fig. 3). The deposition in other areas of metropolitan Phoenix may differ considerably from the deposition in Tempe.

PM_{10} concentration is sometimes reported as 24 h averages instead of 1 h averages. Using 24 h $c(PM_{10})$ data overestimates haboob deposition by 86% (data not shown). The time resolution of a haboob event (1–3 h) is too short to be accurately represented by a 24 h $c(PM_{10})$ value. Employing the haboob particle mass distribution for a full 24 h would erroneously incorporate large particles as a significant fraction of TSP both before and after the haboob events. To avoid such artifacts, we employed 1 h $c(PM_{10})$.

3.4. Dry deposition

The dry deposition flux, J_d, for both PM_{10} and TSP was calculated after making simple assumptions about the particle size distributions present in dust storms and employing a $\frac{PM_{10}}{TSP}$ mass ratio of 0.20. The deposition followed trends in haboob occurrence (see Fig. 8). Most of the haboob deposition occurred during the summer (86%, July to September). Because J_d(TSP) is strongly associated with haboob events, there was a distinct maximum in J_d(TSP) during the summer monsoon period.

The PM_{10} dry deposition flux, $J_d(PM_{10})$, was nearly constant over the course of the year and haboobs contributed very little PM_{10} relative to the background; for example, haboob deposition constituted 21% of overall $J_d(PM_{10})$ in July. The contribution of other dust (events which failed to meet haboob visibility or meteorological criteria) varied somewhat throughout all seasons but was small relative to the calculated background and haboob depositions. Haboob $J_d(PM_{10})$ was much smaller than haboob J_d(TSP) (0.1% for July). This was expected since deposition velocity of particles varies in approximate proportion with the particle diameter squared (see Eq. (1)).

The year-to-year variation in $J_d(PM_{10})$ was small but the year-to-year variation in J_d(TSP) was much greater due to the effect of haboobs (Fig. 9). This was expected since the number and intensity of haboobs varied from year to year. The year 2011 had the highest J_d(TSP), 2950 kg ha^{-1}, of which 92% or 2710 kg ha^{-1} occurred during the 20 haboobs which occurred that year. In contrast, the wettest year, 2010, had the lowest J_d(TSP), 259 kg ha^{-1}, with 23% or 60 kg ha^{-1} of that being deposited in the three haboobs that occurred that year.

On a mass basis, haboob events accounted for 74% of J_d(TSP) but only 5% of $J_d(PM_{10})$, *e.g.*, Fig. 10. In contrast, the urban background particle deposition accounted for 90% of the total $J_d(PM_{10})$ but only 24% of the total J_d(TSP). Most of the deposition mass (98%) was from particles with $d_p > 10$ μm. About 35% of the total deposition occurred during haboobs with $VIS \leqslant 1.6$ km (1 mi) and 39% from haboobs with $1.6 < VIS \leqslant 11.3$ km (1–7 mi; see Fig. S7). In other words, more than a third (333 kg ha^{-1}) of J_d(TSP) was deposited during the most intense quartile of the haboobs (n = 25 out of 96).

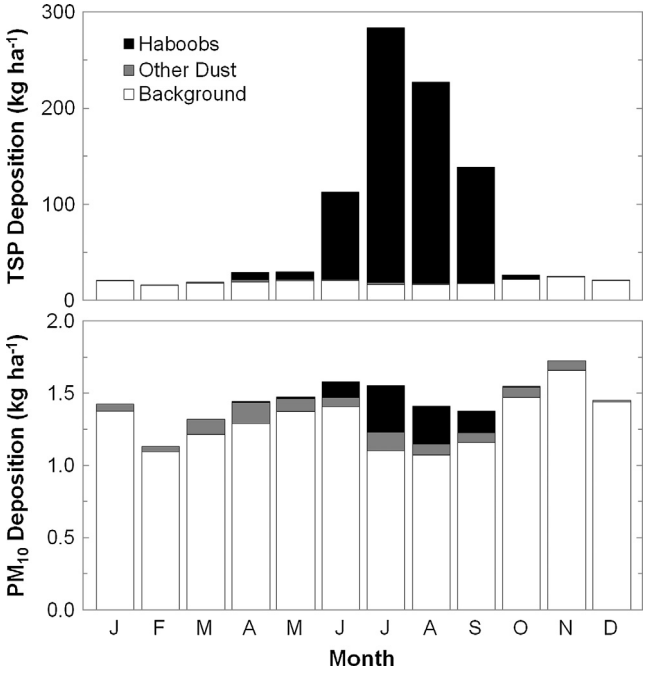

Fig. 8. Mean monthly TSP (top) and PM_{10} (bottom) dry deposition flux (kg ha^{-1}) in Tempe over the period 2005–2014. The haboob contribution to TSP flux is large and occurs only during the summer. PM_{10} flux is a very small fraction of TSP flux and is relatively constant throughout the year. Note the two orders of magnitude difference in the deposition scales.

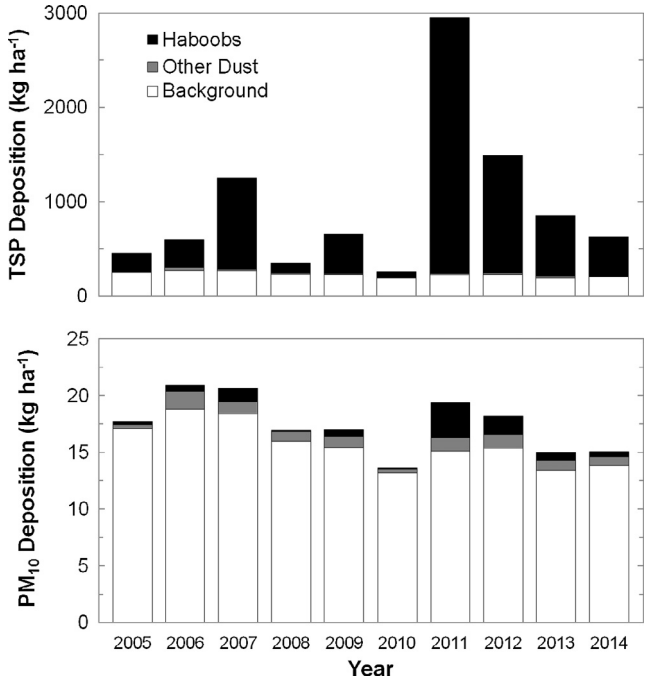

Fig. 9. Annual TSP (top) and PM_{10} (bottom) dry deposition flux (kg ha^{-1}) in Tempe from 2005 to 2014. The haboob contribution to TSP flux is variable and depends on both on the number and magnitude of events.

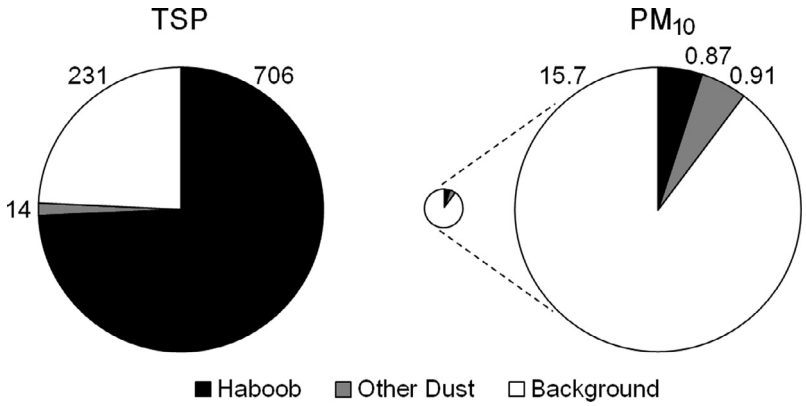

Fig. 10. Mean annual dry deposition (kg ha^{-1} yr^{-1}) in Tempe for the period 2005–2014. The TSP deposition (left) and the PM_{10} deposition (right) for haboobs, other dust and background time periods. The numbers are the deposition quantities in kg ha^{-1} yr^{-1}. The area of the small PM_{10} pie chart is scaled proportionally to the TSP deposition pie chart for comparison.

The J_d(TSP) calculated in this work (mean: 950 kg ha^{-1} yr^{-1}) was similar in magnitude to deposition fluxes reported in the literature (see Table 2). During a particularly rainy year (355 mm precipitation) in metropolitan Phoenix, Péwé et al. (1981), reported a rooftop J_d(TSP) = 540 kg ha^{-1} yr^{-1}, 12% of which was attributed to two haboobs. This compares with the relatively wet year (2010) in this study, with 232 mm rain and J_d(TSP) = 259 kg ha^{-1} yr^{-1}, 23% being deposited in three haboobs. Excluding haboob deposition, the J_d(TSP) of the sum of background and other blowing dust ranged from 199 to 299 kg ha^{-1} yr^{-1} with a mean of 244 kg ha^{-1} yr^{-1}. Smaller J_d(TSP) of 20–200 kg ha^{-1} yr^{-1} has been reported in Southern California and Nevada, where haboobs did not occur (Reheis, 2006). There was only one year where J_d(TSP) was calculated to be higher than deposition reported in some locations of northern Africa: 2011 with J_d(TSP) = 2950 kg ha^{-1} yr^{-1}. In 2011, there were 20 haboobs – the highest in the present work. The estimated 2950 kg ha^{-1} yr^{-1} was less than the deposition of 6940 kg ha^{-1} reported in a series of dust storms over a period of four weeks in the Ukraine (Shikula, 1981), less than the 6140 kg ha^{-1} yr^{-1} reported in New Zealand (McGowan et al., 1996), and less than the deposition of 4210 kg ha^{-1} yr^{-1} reported in Waddan, Libya (O'Hara et al., 2006). A single haboob in western Texas (Chen and Fryrear, 2002) was reported to deposit 850 kg ha^{-1} h^{-1}, which was higher than any single haboob identified in the present study, the highest being 362 kg ha^{-1} h^{-1} during the 30 June 2013 haboob (maximum $c(PM_{10})$ = 5250 μg m^{-3}; minimum VIS = 1.2 km (0.75 mi); maximum v_{WG} = 21 m s^{-1} (47 mi h^{-1})). The large variation in values of J_d(TSP) reported for sites throughout the world (Table 2) is probably a reflection of real differences in dust storm intensity, type, and frequency; in that context, the range of predicted annual J_d(TSP) magnitudes in this study was not surprising. The deposition values calculated within this study were consistent with literature data in arid environments. The recent Vukovic et al. (2014) study also concluded that the models need to better account for the effects of the very largest particle sizes and our results further amplify the need for improved monitoring of large particle sizes.

4. Conclusions

We cataloged the occurrence of haboobs over the time period 2005–2014 using a method based on meteorological and air quality measurements. The major factors that distinguish haboobs events from other dust events and background conditions were event minimum visibility, maximum wind or gust speed, and maximum PM_{10} concentration. This work represents a necessary first step in determining the ecological impact of dust deposition in the Phoenix metropolitan region.

There were between three and 20 haboob events per year, with a somewhat lower number of haboob events occurring in years with higher annual precipitation. The relationship between precipitation and haboob occurrence is complex due to the bimodality of seasonal precipitation as well as the mutual source of haboobs and monsoon precipitation. There was a strong seasonal pattern in haboob occurrence with the majority of haboobs occurring during the North American monsoon season (*i.e.*, June to September) and no events occurring in the winter.

The calculated PM dry deposition in Tempe compares well with literature deposition reported for other arid environments when haboob deposition is included in the model. Annual J_d(TSP) ranged from a low of 259 kg ha^{-1} in 2010 to a high of 2950 kg ha^{-1} in 2011. The contribution of large particles ($PM_{>10}$) is greater than the contribution of PM_{10} to deposition: the average annual J_d(TSP) was 950 kg ha^{-1} yr^{-1} while $J_d(PM_{10})$ was 17 kg ha^{-1} yr^{-1}. Our haboob mass distribution was compiled from literature studies, many of which provided only partial information across the range of particle sizes in the deposition model. Thus, there is a need to measure the TSP mass distribution in metropolitan Phoenix.

This study characterized haboobs at a single location in metropolitan Phoenix in an effort to minimize the spatio-temporal heterogeneity of haboobs. There is a continued need to investigate the spatial differences in haboobs throughout metropolitan Phoenix and in surrounding areas. There may also be a need to investigate meteorological and air quality characteristics in the desert to the south where measurements are currently quite limited.

Acknowledgments

This material is based upon work supported by the National Science Foundation [grant number BCS-1026865, Central Arizona-Phoenix Long-Term Ecological Research (CAP LTER)]. This work was also partially funded by SRP. Any opinions, findings, and conclusions or recommendations expressed in this material are those of the author(s) and do not necessarily reflect the views of the funding agencies.

Appendix A. Supplementary material

Supplementary data associated with this article can be found, in the online version, at http://dx.doi.org/10.1016/j.aeolia.2016.11.

004. These data include Google maps of the most important areas described in this article.

References

Arizona Department of Environmental Quality (ADEQ), 2015. ADEQ Air Quality Division: Natural and Exceptional Events <https://www.azdeq.gov/environ/air/plan/nee.html> (accessed 12.02.15).

Ball, B.A., Alvarez Guevara, J., 2015. The nutrient plasticity of moss-dominated crust in the urbanized Sonoran Desert. Plant Soil 389 (1), 225–235. http://dx.doi.org/10.1007/s11104-014-2355-7.

Bateman, H.L., Stromberg, J.C., Banville, M.J., Makings, E., Scott, B.D., Suchy, A., Wolkis, D., 2015. Novel water sources restore plant and animal communities along an urban river. Ecohydrology 8 (5), 792–811. http://dx.doi.org/10.1002/eco.1560.

Box, M.A., Radhi, M., Box, G.P., 2010. The great Sydney dust event: size-resolved chemical composition and comparison. In: 17th National Conference of the Australian Meteorological and Oceanographic Society. IOP Conf. Ser.: Earth and Environ. Sci. 11(1), 012015. http://dx.doi.org/10.1088/1755-1315/11/1/012015.

Brazel, A.J., 1989. Dust and climate in the American southwest. In: Leinen, M., Sarnthein, M. (Eds.), Paleoclimatology and Paleometeorology: Modern and Past Patterns of Global Atmospheric Transport. NASA ASI Series C, vol. 282. Kluwer Academic Publishers, Dordrecht, pp. 65–96. ISBN: 978-94-009-0995-3.

Brazel, A.J., Nickling, W.G., 1986. The relationship of weather types to dust storm generation in Arizona (1965–1980). J. Climatol. 6 (3), 255–275. http://dx.doi.org/10.1002/joc.3370060303.

Chen, W., Fryrear, D.W., 2002. Sedimentary characteristics of a haboob dust storm. Atmos. Res. 61 (1), 75–85. http://dx.doi.org/10.1016/S0169-8095(01)00092-8.

Chepil, W.S., 1957. Sedimentary characteristics of dust storms—III. Composition of suspended dust. Am. J. Sci. 255 (3), 206–213. http://dx.doi.org/10.2475/ajs.255.3.206.

Chepil, W.S., Woodruff, N.P., 1957. Sedimentary characteristics of dust storms—II. Visibility and dust concentration. Am. J. Sci. 255 (2), 104–114. http://dx.doi.org/10.2475/ajs.255.2.104.

Clements, A.L., Fraser, M.P., Herckes, P., Solomon, P.A., 2016. Chemical mass balance source apportionment of fine and PM10 in the Desert Southwest, USA. AIMS Environ. Sci. 3 (1), 115–132. http://dx.doi.org/10.3934/environsci.2016.1.115.

Clements, A.L., Fraser, M.P., Upadhyay, N., Herckes, P., Sundblom, M., Lantz, J., Solomon, P.A., 2013. Characterization of summertime coarse particulate matter in the Desert Southwest-Arizona, USA. J. Air Waste Manage. Assoc. 63 (7), 764–772. http://dx.doi.org/10.1080/10962247.2013.787955.

Clements, A.L., Fraser, M.P., Upadhyay, N., Herckes, P., Sundblom, M., Lantz, J., Solomon, P.A., 2014. Chemical characterization of coarse particulate matter in the Desert Southwest – Pinal County Arizona, USA. Atmos. Pollut. Res. 5 (1), 52–61. http://dx.doi.org/10.5094/APR.2014.007.

Davis, M.K., Cook, E.M., Collins, S.L., Hall, S.J., 2015. Top-down vs. bottom-up regulation of herbaceous primary production and composition in an arid, urbanizing ecosystem. J. Arid Environ. 116, 103–114. http://dx.doi.org/10.1016/j.jaridenv.2015.01.018.

Drees, L.R., Manu, A., Wilding, L.P., 1993. Characteristics of aeolian dusts in Niger, West Africa. Geoderma 59, 213–233. http://dx.doi.org/10.1016/0016-7061(93)90070-2.

Gillette, D.A., Clayton, R.N., Mayeda, T.K., Jackson, M.L., Sridhar, K., 1978. Tropospheric aerosols from some major dust storms of the southwestern United States. J. Appl. Meteor. 17 (6), 832–845. http://dx.doi.org/10.1175/1520-0450.

Giraudeau, M., Chavez, A., Toomey, M.B., McGraw, K.J., 2015. Effects of carotenoid supplementation and oxidative challenges on physiological parameters and carotenoid-based coloration in an urbanization context. Behav. Ecol. Sociobiol. 69 (6), 957–970. http://dx.doi.org/10.1007/s00265-015-1908-y.

Goossens, D., Offer, Z.Y., 1995. Composition of day-time and night-time dust accumulation in a desert region. J. Arid Environ. 31 (3), 253–281. http://dx.doi.org/10.1016/S0140-1963(05)80032-1.

Goudie, A.S., 1983. Dust storms in space and time. Prog. Phys. Geogr. 7, 502–530. http://dx.doi.org/10.1177/030913338300700402.

Goudie, A.S., Middleton, N.J., 2000. Dust storms in South West Asia. Acta Univ. Car. XXXV, 73–83.

Hagen, L., Woodruff, N., 1973. Air pollution from duststorms in the Great Plains. Atmos. Environ. 7, 323–332. http://dx.doi.org/10.1016/0004-6981(73)90081-4.

Holcombe, T.L., Ley, T., Gillette, D.A., 1997. Effects of prior precipitation and source area characteristics on threshold wind velocities for blowing dust episodes, Sonoran Desert 1948–78. J. Appl. Meteor. 36, 1160–1175. http://dx.doi.org/10.1175/1520-0450(1997) 036∗1160:EOPPAS∗2.0.CO;2.

Huffington Post, 2011. Phoenix Dust Storm: Arizona Hit with Monstrous 'Haboob'. Huffington Post, Posted: Jul 6, 2011. <http://www.huffingtonpost.com/2011/07/06/Phoenix-dust-storm-photos-video_n_891157.html> (accessed 11.20.15).

Hyers, A.D., Marcus, M.G., 1981. Land use and desert dust hazards in central Arizona. Geol. Soc. Am. Spec. Pap. 186, 267–280. http://dx.doi.org/10.1130/SPE186-p267.

Idso, S.B., 1976. Dust storms. Sci. Am. 235, 108–114. http://dx.doi.org/10.1038/scientificamerican1076-108.

Idso, S.B., Ingram, R., Pritchard, J., 1972. An American haboob. Bull. Am. Meteor. Soc. 53, 930–935. http://dx.doi.org/10.1175/1520-0477(1972) 053∗0930:AAH∗2.0.CO;2.

Jenerette, G.D., Wu, J., 2001. Analysis and simulation of land-use change in the central Arizona – Phoenix region, USA. Landsc. Ecol. 16 (7), 611–626. http://dx.doi.org/10.1023/A:1013170528551.

Joseph, P.V., 1982. A tentative model of Andhi. Mausam 33, 417–422.

Joseph, P.V., Raipal, D.K., Deka, S.N., 1980. Andhi, the convective dust-storm of northwest India. Mausam 31, 431–442.

Lawrence, C.R., Neff, J.C., 2009. The contemporary physical and chemical flux of aeolian dust: a synthesis of direct measurements of dust deposition. Chem. Geol. 267 (1–2), 46–63. http://dx.doi.org/10.1016/j.chemgeo.2009.02.005.

Lei, H., Wang, J.X.L., 2014. Observed characteristics of dust storm events over the western United States using meteorological, satellite, and air quality measurements. Atmos. Chem. Phys. 14 (15), 7847–7857. http://dx.doi.org/10.5194/acp-14-7847-2014.

Li, X., Myint, S.W., Zhang, Y., Galletti, C., Zhang, X., Turner II, B.L., 2014. Object-based land-cover classification for metropolitan Phoenix, Arizona, using aerial photography. Int. J. Appl. Earth Obs. Geoinf. 33, 321–330. http://dx.doi.org/10.1016/j.jag.2014.04.018.

Macpherson, T., Nickling, W.G., Gillies, J.A., Etyemezian, V., 2008. Dust emissions from undisturbed and disturbed supply-limited desert surfaces. J. Geophys. Res. 113, F02S04. http://dx.doi.org/10.1029/2007JF000800.

Maley, J., 1980. Etudes palynologiques dans le bassin du Tchad et Paléoclimatologie de l'Afrique nord tropicale de 30.000 ans à 1'époque actuelle (Thesis). Université de Montpellier, France.

Maricopa County Assessor's Office, 2016. Maps: Historical Aerial Photography <http://gis.maricopa.gov/MapApp/GIO/AerialHistorical/index.html> (accessed 06.03.16), Single aerial maps for years 1976 and 2013.

Mathematica, 2015a. Mathematica version 10.2.0.0; function ThermodynamicData ["Air", "Viscosity",{"Pressure", "Temperature"}]; Wolfram Research: Champaign, IL.

Mathematica, 2015b. Mathematica version 10.2.0.0; function ThermodynamicData ["Air", "Density",{"Pressure", "Temperature"}]; Wolfram Research: Champaign, IL.

McGowan, H.A., Sturman, A.P., Owens, I.F., 1996. Aeolian dust transport and deposition by foehn winds in an Alpine environment, Lake Tekapo, New Zealand. Geomorphology 15 (2), 135–146. http://dx.doi.org/10.1016/0169-555X(95)00123-M.

McTainsh, G.H., 1980. Harmattan dust deposition in northern Nigeria. Nature 286 (5773), 587–588. http://dx.doi.org/10.1038/286587a0.

Membery, D.A., 1985. A gravity wave haboob? Weather 40, 214–221. http://dx.doi.org/10.1002/j.1477-8696.1985.tb06877.x.

MesoWest, 2015. Department of Atmospheric Sciences. University of Utah. <http://mesowest.utah.edu/cgi-bin/droman/download_ndb.cgi> (accessed 07.02.15).

Miller, E.R., 1934. Meteorology of the dust fall of November 12–13, 1933. J. Sedimentary Res. 4 (2), 78–81. http://dx.doi.org/10.1306/D4268EBE-2B26-11D7-8648000102C1865D.

Miller, S.D., Kuciauskas, A.P., Liu, M., Ji, Q., Reid, J.S., Breed, D.W., Walker, A.L., Mandoos, A.A., 2008. Haboob dust storms of the southern Arabian Peninsula. J. Geophys. Res. 113, D01202. http://dx.doi.org/10.1029/2007JD008550.

Møberg, J.P., Esu, I.E., Malgwi, W.B., 1991. Characteristics and constituent composition of Harmattan dust falling in northern Nigeria. Geoderma 48 (1–2), 73–81. http://dx.doi.org/10.1016/0016-7061(91)90007-G.

Nickling, W.G., Brazel, A.J., 1984. Temporal and spatial characteristics of Arizona dust storms (1965–1980). J. Climatol. 4 (6), 645–660. http://dx.doi.org/10.1002/joc.3370040608.

O'Hara, S.L., Clarke, M.L., Elatrash, M.S., 2006. Field measurements of desert dust deposition in Libya. Atmos. Environ. 40, 3881–3897. http://dx.doi.org/10.1016/j.atmosenv.2006.02.020.

O'Loingsigh, T., McTainsh, G.H., Tews, E.K., Strong, C.L., Leys, J.F., Shinkfield, P., Tapper, N.J., 2014. The Dust Storm Index (DSI): a method for monitoring broadscale wind erosion using meteorological records. Aeolian Res. 12, 29–40. http://dx.doi.org/10.1016/j.aeolia.2013.10.004.

Orgill, M.M., Sehmel, G.A., 1976. Frequency and diurnal variation of dust storms in the contiguous U.S.A. Atmos. Environ. 10 (10), 813–825. http://dx.doi.org/10.1016/0004-6981(76)90136-0.

Péwé, T.L., Péwé, E.A., Péwé, R.H., Journaux, A., Slatt, R.M., 1981. Desert Dust: characteristics and rates of deposition in central Arizona. Geol. Soc. Am. Spec. Pap. 186, 169–190. http://dx.doi.org/10.1130/SPE186-p169.

Raman, A., Arellano, A.F., Brost, J.J., 2014. Revisiting haboobs in the southwestern United States: an observational case study of the 5 July 2011 Phoenix dust storm. Atmos. Environ. 89, 179–188. http://dx.doi.org/10.1016/j.atmosenv.2014.02.026.

Reheis, M.C., 2006. A 16-year record of eolian dust in southern Nevada and California, USA: controls on dust generation and accumulation. J. Arid Environ. 67 (3), 487–520. http://dx.doi.org/10.1016/j.jaridenv.2006.03.006.

Roberts, A., Knippertz, P., 2012. Haboobs: convectively generated dust storms in West Africa. Weather 67 (12), 311–316. http://dx.doi.org/10.1002/wea.1968.

Sauret, N., Wortham, H., Strekowski, R., Herckes, P., Nieto, L.I., 2009. Comparison of annual dry and wet deposition fluxes of selected pesticides in Strasbourg, France. Environ. Pollut. 157 (1), 303–312. http://dx.doi.org/10.1016/j.envpol.2008.06.034.

Seinfeld, J.H., Pandis, S.N., 2006. Atmospheric Chemistry and Physics: From Air Pollution to Climate Change, Ed 2; Wiley, Hoboken, New Jersey, pp. 400–422. ISBN: 978-0-471-72018-8.

Shikula, N.K., 1981. Prediction of dust storms from meteorological observations in the South Ukraine, U.S.S.R. Geol. Sot. Am. Spec. Pap. 186, 261–266. http://dx.doi.org/10.1130/SPE186-p261.

Singer, A., Ganor, E., Dultz, S., Fischer, W., 2003. Dust deposition over the Dead Sea. J. Arid Environ. 53 (1), 41–59. http://dx.doi.org/10.1006/jare.2002.1023.

Sorooshian, A., Wonaschütz, A., Jarjour, E.G., Hashimoto, B.I., Schichtel, B.A., Betterton, E.A., 2011. An aerosol climatology for a rapidly growing arid region (southern Arizona): major aerosol species and remotely sensed aerosol properties. J. Geophys. Res. 116, D19205. http://dx.doi.org/10.1029/2011JD016197.

Sutton, L.J., 1925. Haboobs. Q. J. R. Meteorol. Soc. 51, 25–30. http://dx.doi.org/10.1002/qj.49705121305.

Upadhyay, N., Clements, A.L., Fraser, M.P., Sundblom, M., Solomon, P., Herckes, P., 2015. Size-differentiated chemical composition of re-suspended soil dust from the desert southwest United States. Aerosol Air Qual. Res. 15 (2), 387–398. http://dx.doi.org/10.4209/aaqr.2013.07.0253.

U.S. Census Bureau, 2013. Metropolitan and Micropolitan: Population Change for Metropolitan and Micropolitan Statistical Areas in the United States and Puerto Rico (February 2013 Delineations): 2000 to 2010. <http://www.census.gov/population/www/cen2010/cph-t/cph-t-5.html> (accessed 11.24.15).

U.S. Environmental Protection Agency (EPA), 2006. The treatment of data influenced by exceptional events. Proposed Rule. Fed. Regist. 71 (47), 12592–12610.

U.S. Environmental Protection Agency (EPA), 2007. Treatment of data influenced by exceptional events. Final Rule. Fed. Regist. 72 (55), 13560–13581.

U.S. Environmental Protection Agency (EPA), 2013. National ambient air quality standards for particulate matter: final rule. Fed. Regist. 78 (10), 3085–3287.

U.S. Environmental Protection Agency (EPA), 2015. AirData: Query AirData. <https://aqs.epa.gov/api> (accessed 07.02.15).

U.S. National Oceanic and Atmospheric Administration (NOAA), 2015. National Centers for Environmental Information: Quality Controlled Local Climatological Data, version 2.5.10. http://www.ncdc.noaa.gov/qclcd/QCLCD?prior=N (accessed 07.02.15).

U.S. National Weather Service (NWS), 2016. NWS Phoenix: Monsoon Awareness Week: June 12th–17th, 2016. <http://www.wrh.noaa.gov/psr/pns/2016/June/MonsoonAwarenessWeek.php> (accessed 06.15.16).

Vukovic, A., Vujadinovic, M., Pejanovic, G., Andric, J., Kumjian, M.R., Djurdjevic, V., Dacic, M., Prasad, A.K., El-Askary, H.M., Paris, B.C., Petkovic, S., Nickovic, S., Sprigg, W.A., 2014. Numerical simulation of "an American haboob". Atmos. Chem. Phys. 14, 3211–3230.

Warn, G.F., Cox, W.H., 1951. A sedimentary study of dust storms in the vicinity of Lubbock, Texas. Am. J. Sci. 249 (8), 553–568. http://dx.doi.org/10.2475/ajs.249.8.553.

World Health Organization (WHO), 2006. Air Quality Guidelines. Global update 2005. Particulate Matter, Ozone, Nitrogen Dioxide and Sulfur Dioxide. WHO Regional Office for Europe; Copenhagen. <http://www.euro.who.int/__data/assets/pdf_file/0005/78638/E90038.pdf?ua=1> (accessed 12.22.15). ISBN 92-890-2192-6.